Helmet Standoff Variation on Human Heads

Erika Matheis[1], Karin Rafaels

[1]Bennett Aerospace 1 GLENWOOD AVENUE, 5TH FLOOR RALEIGH, NORTH CAROLINA 27603 USA
erika.a.matheis.ctr@army.mil
410-306-4970

Abstract: Behind-helmet blunt trauma (BHBT) can occur when a threat is defeated by the helmet, but the helmet deformation exceeds the standoff distance between the helmet and the head. Previous research has demonstrated that effects are sensitive to standoff [1-5]. However, the standoffs that have been used in various assessments and studies are not consistent: 12.7 and 19.1mm to represent pad thickness [1], 22 mm from the ISO "J" headform [2]; and 14.9 mm in a study using the Ballistic Load Sensing Headform (BLSH) [3]. In a computational modeling study, large differences in injury risk were identified when the standoff was varied by 3 mm [2]. Therefore, assessments using different standoffs may not predict the same injury risk for identical helmet impacts. Consequently, helmet testing should examine fit and standoff more closely to ensure that unrealistic loading conditions are not being used in helmet evaluation tests. This study examines the helmet fit on human heads to provide insights on standoffs to inform laboratory testing methods. A single helmet geometry was fitted onto 25 human heads and scanned using computed tomography. Three-dimensional renderings of the helmet and head were created and analysed to determine the standoff between the helmet and the skin beneath. The standoff distribution for all 25 heads was normal with an average standoff of 24.1 ± 4.5 mm, with a range that spans 32.6 mm. Within each individual, the range was not as large as the whole population, but still spanned between 14.3 mm for the densest distribution and was as large as 27.6 mm for the widest distribution of standoffs. The median for 52% of the individuals was greater than the average standoff for the entire study, which means that more than half of the individual's measured standoffs were greater than the average. The wide range of standoffs measured between the head and helmet suggests that a single standoff for laboratory testing may not accurately represent the risk for injury behind helmets. Understanding the range and variance of standoff values in human heads may provide better insight for injury risk and potentially relevant standoffs to be used in test methods.

1. INTRODUCTION

With the increase in threats for law enforcement officers, ballistic head protection is suggested for scenarios when units are called upon to neutralise a situation [6]. Behind-helmet blunt trauma (BHBT) can occur in law enforcement tactical operations, where a threat is defeated by the helmet, but the deformation exceeds the standoff distance between the helmet and the head. This phenomenon is linked to some potentially serious injuries [4, 7-9]. Therefore, it is important to consider this injury mechanism in ballistic helmet test evaluations.

Standoff is important because it allows the helmet to dissipate more energy through deformation before contacting the head [2, 4, 10, 11]. In previous studies, there is not a consistent value for tested standoff, nor a consistent headform [1-3, 7, 12]. The different standoffs that have been used range from 12.5-25 mm [1, 7, 10, 12, 13]. Because of the lack of standardisation of standoff, there may be differences in the predicted injury effects through energy transfer. There are anthropometric differences of head shape within a human population and even some differences between standardised headforms. While headforms may be modelled after a human population [14], there are inherent differences. One headform used the "average skull" from a sample of 16 average-sized Western adults to determine its shape while the others have unknown origins of the original anthropometric dataset [15]. Some other headforms that are used for ballistic testing standards have no clear anthropometric origin and were developed for a specific test methodology [5]. Headforms may also have the same circumference measurement, but have different head breadth, length, and height measurements [14], which would change surface curvature and standoff values when helmeted. Some helmet studies have noted difficulties and performance differences with helmet fitting due to geometric differences [12, 16]. Previous research has recognised the importance of anthropometric differences and have characterised human head 3D measurements for helmet fitting and design [17-20], however standoff variation was not measured. The variance in standoff distances is unknown in a human population. Standoff variation is a known issue for helmet testing [5] and testing a single standoff may lead to unrealistic energy transfer predictions through BHBT for the

https://doi.org/10.52202/080042-0014

helmet-wearing population. This research investigates the range of standoffs within a human dataset to give insights for testing methods.

2. MATERIALS AND METHODS

2.1. Helmet Fitting and Image Acquisition

Twenty-five fresh-frozen post-mortem human subject (PMHS) heads, sectioned at the atlanto-occipital joint, were used in this study. Anthropometric measurements were taken to measure head length, breadth and circumference using calipers and tailor's tape. All specimens were fit into the same make, model, and size helmet. The suspension system was tightened so the helmet was level from side to side and stable when attempting to rock the helmet on the head. The front rim of the helmet was positioned just above the brow ridge. The head donned with the helmet was then CT-scanned using a defined protocol of 140 kVp, 250 mA, and a slice thickness of 0.625 mm.

The PMHS heads were purchased through a licensed and certified vendor of human tissue: Science Care, Inc., (21410 N 19th Ave, Suite 126, Phoenix, AZ 85027). Criteria for acceptable specimens included: male specimens without known previous or existing skull malformations and surgical procedures or interventions; fitting into the same size helmet; and approximately 50% in size for the male population. All handling and testing of the PMHS specimens were done in accordance with the Combat Capabilities Development Command (DEVCOM) Army Research Laboratory's (ARL) Policy for Use of Human Cadavers for Research, Development, Test, and Evaluation (RDT&E) under the guidance and oversight of the DEVCOM ARL Human Cadaver Review Board and the DEVCOM ARL Safety Office.

2.2. Image Segmentation and Post-processing

The images were analysed using Mimics (version 24, Materialise, Leuven, Belgium). The helmet was masked to a Housfield unit (HU) threshold of -200 to 200 HU; and holes were filled in where necessary (i.e. for equipment that may be mounted to the helmet or missing areas due to artifact). The soft tissue was masked to a threshold of -700 to 200 HU; and the skull was masked to the "bone" setting (226 HU to 3071 HU). The different masks were made into individual parts and then the parts were smoothed while compensating for shrinkage using 20 iterations with a smooth factor of 0.9. To improve rendering and reduce memory requirements, a triangle reduction of the parts was performed in edge mode with a 0.03 mm tolerance and 15-degree edge angle for 10 iterations. Finally, a wrapping surface was applied to the parts to filter out small inclusions and close any remaining small holes defined using the size of the new triangles, or the smallest detail, to be 1 mm and a gap-closing distance of 1 mm.

The STL parts were exported from Mimics to 3-matic (version 16) for standoff analysis. To define the helmet surface used for the standoff analysis, the helmet was sectioned to include only regions of interest. In this study, since the standoff is considered from the inside surface of the helmet, the helmet was sectioned to only include the inner surface closest to the head. As communication devices and ear protection can vary among users and ballistic helmets have varying degrees of coverage over the ears, this analysis did not include areas in and around the ears (Figure 1). Because some helmets have different brim and rim geometries, 20 mm of the helmet was removed at the front and back edge of the helmet to avoid issues with those components. The area around the attachment points of the retention or suspension system was also not included in this analysis since retention and suspension systems attachments vary. Once the final inner helmet surface area with only the regions of interest included, the final surface and part was reduced to 7,000-8,000 triangles. For the head, where there was an artifact or defect on the skin, the skin surface was locally smoothed. Once revised, the outer skin surface was defined as a part.

https://doi.org/10.52202/080042-0014

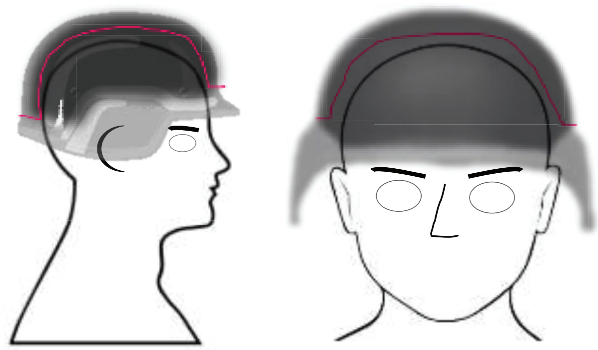

Figure 1: General geometry of a helmet with earflaps and a brim on head as worn (light gray), where the darker region (dark gray) was the approximate geometry assessed leaving out the earflaps and brim. The pink line represents a general inner surface of the helmet that was assessed for the differences between the head and helmet for the standoff measurement in the 3D viewing software.

To obtain the standoff between the helmet inner surface part and the skin outer surface part, the part comparison function in 3-matic was used. This function analyses the differences between two parts and outputs a point-cloud of coordinates and distances between parts. These calculated distances were then exported into JMP 14 (SAS, Cary, NC) for further analysis. The 25 different helmets and heads resulted in files with 3,200-6,000 standoff datapoints.

2.3. Data Analysis

Using JMP 14, descriptive statistics for all standoffs from each helmet and head combined were calculated, including the mean, standard deviation, median, quartiles, and range. A continuous best-fit density curve was generated where the Akaike Information Criterion (AICc) (Equation 1) was used to choose the best fit of a statistical model. This formula uses the number of estimated parameters (k) and the number of observations (n) used in the model. The lower the value, the better the fit when comparing multiple different options. There were a few standard options that JMP populates including comparisons with normal, normal mixtures, lognormal, Weibull, extreme value, Johnson, gamma, Sinh-Arcsinh, and exponential.

$$AICc = -2LogLikelihood + 2k + 2k(k+1) /(n-k-1) \quad (1)$$

Per specimen values for mean, standard deviation, median, quartiles and range were calculated for standoffs and head anthropometry. Individual distribution characteristics were explored through modality, kurtosis, skewness and density curve fit. A continuous best-fit curve was picked using the AIC for each individual to assess different characteristics across the dataset. Individual means were then also compared with each other to assess significant differences between individuals using a one-way analysis of variance (ANOVA) with post-hoc Tukey honest significant difference (HSD).

3. RESULTS

3.1. Total Population Standoff

Using all collected datapoints from the 25 heads, the standoff distribution was normal. In Figure 2, the total dataset looks like a normal distribution, however there are over 104,000 datapoints which may settle into a normal distribution because of the high density of datapoints across a range. The average standoff was 24.1 ± 4.5 mm with a median that matched the average (24.1 mm). Values from the 25-75% quartiles ranged from 21.1 mm to 27.1 mm, with only a 6 mm difference. The total range spanned 32.6 mm. When a best continuous-fit density curve was calculated for the total dataset, it fit a normal 3 mixture curve with an AICc of 609615 where other fitted curves tested were 204 greater than the chosen best fit. A lower AICc indicates a better fit of the model based on the likelihood probability. The normal 3 mixture model has 3 separate locations for the mean and 3 separate dispersions for the standard deviation, indicating that the numbers come from 3 separate populations. If you increase the parameter numbers to a fitted normal 25 mixture (the total population size) the AICc decreases by 557, indicating a better fit. This is to be expected because the more parameters included in a model, the better fit for the curve.

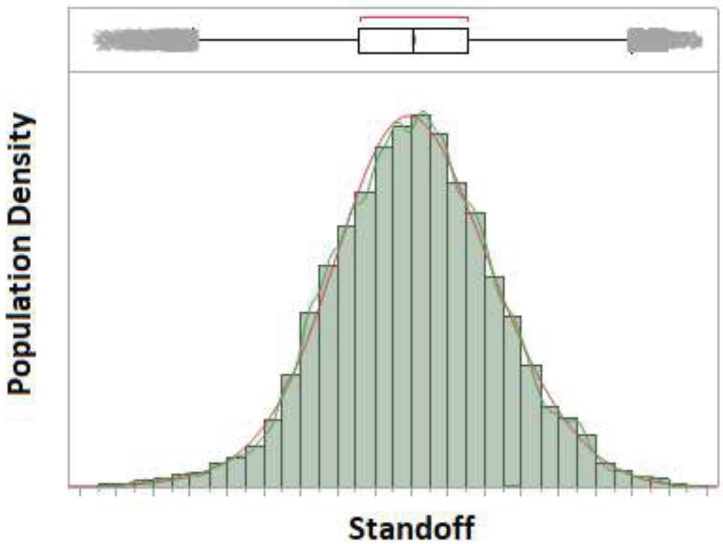

Figure 2: Total dataset distribution of standoffs. Red curve fit is a normal 3 mixture density curve and green is a normal 25 mixture density curve (matching population size). Boxplot at the top of the graph represents the spread of data where the centre line is the 50% median, the middle of the diamond is the sample mean with top and bottom indicating a 95% confidence interval, the whisker edges represent the furthest point within 1.5 times the interquartile range from the box, and the red bracket represents the densest part of the dataset that encompasses 50% of the data.

3.2. Individual Standoff

When comparing each individual distribution, 84% of the population had a unimodal distribution of standoffs and 16% of the population had bimodal distributions (Figure 3). The individuals with bimodal distributions (4 total) were included in the evaluation of skewness but were excluded from kurtosis analysis. There was variance in skewness for individuals, where 28% of individuals were less than 0.1 askew. The median for 52% of the individuals was greater than the average standoff for the entire study, which means that more than half of the individual's measured standoffs were greater than the average. Furthermore, the distributions of 68% of individuals was negatively skewed, indicating that the means of these individuals underestimate the most common standoffs seen in that individual. Evaluating the kurtosis of individual distributions identified only 2 individuals with a positive (leptokurtic) distribution, which suggests that these individuals had a higher likelihood of extreme standoffs. These two individuals also had the most extreme values of skewness in the positive direction (right skew), which may contribute to the positive kurtosis values. The other 90% of the individuals leaned toward a negative (platykurtic) distribution which denotes a flatter distribution with more standoffs centred around the mean.

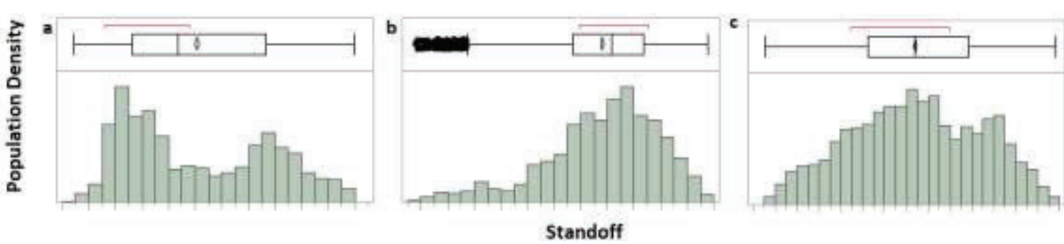

https://doi.org/10.52202/080042-0014

Figure 3:a) An example of a biomodal distribution with two clear peaks in data. b) An example of a negative skew (left skew) of datapoints indcating more collected data is more than the mean, and a leptokurtic distribution, with more extreme values. c) An example of a platykurtic distribution which is a flatter distribution. Boxplot at the top of the graph represents the spread of data where the centre line is the 50% median, the middle of the diamond is the sample mean with top and bottom indicating a 95% confidence interval, the whisker edges represent the furthest point within 1.5 times the interquartile range from the box, and the red bracket represents the densest part of the dataset that encompasses 50% of the data.

Continuous best-fit density curves were fit to each individual dataset by comparing the AICc values and the normal 3 mixture (8 parameters) had the best fit for 84% of the population, where 12% had a normal 2 mixture (5 parameters) for the best fit and only one participant (remaining 4%) had a Sinh-Arcsinh (SHASH) distribution (4 parameters) best fit (Figure 4). A normal 3 mixture curve fit represents a mixture of 3 different regions of more frequent standoffs (Figure 4), where a normal 2 mixture curve fit represents two regions of more frequent standoffs. These density curves indicate that 96% of the individuals evaluated in this study may have different regions around which standoff is distributed. A SHASH distribution identifies asymmetry and/or tails that are lighter than the normal as indicated by one individual and fits a single peak distribution curve.

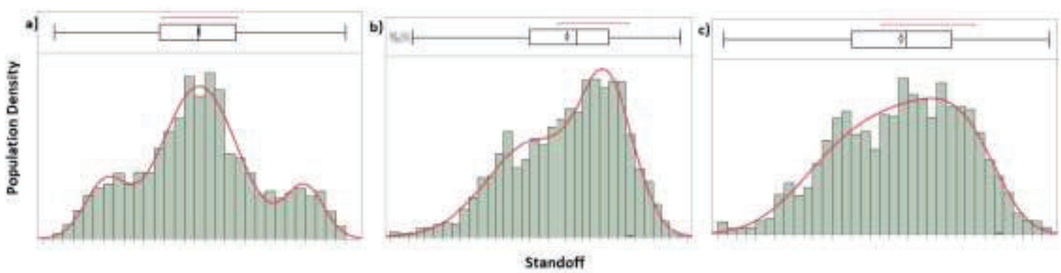

Figure 4: a) An example of a normal 3 mixture curve fit, which would represent a mixture of 3 different frequent standoffs as seen by the three peaks. b) An example of a normal 2 mixture curve fit, which would represent a mixture of 2 frequent standoffs as seen by the two peaks. c) An example of a SHASH distribution which identifies asymmetry and/or tails that are lighter than the normal. Boxplot at the top of the graph represents the spread of data where the centre line is the 50% median, the middle of the diamond is the sample mean with top and bottom indicating a 95% confidence interval, the whisker edges represent the furthest point within 1.5 times the interquartile range from the box, and the red bracket represents the densest part of the dataset that encompasses 50% of the data.

Within each individual, the range was not as large as the whole population, but still spanned between 14.3 mm for the densest distribution and was as large as 27.6 mm for the widest distribution of standoffs. The mean range of standoff within each individual was 19.62 ± 3.60 mm. The median range was less than the mean at 19.40 mm with 22.45 mm at 75% quartile and 16.70 mm at the 25% quartile. The range of standoff skewed toward a smaller range than the average (Figure 5).

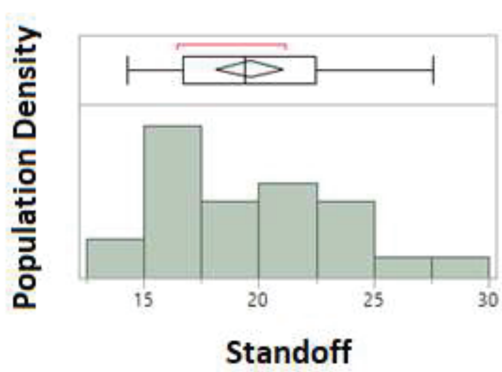

Figure 5: Range of standoff per individual in millimetres. Boxplot at the top of the graph represents the spread of data where the centre line is the 50% median, the middle of the diamond is the sample mean with top and bottom indicating a 95% confidence interval, the whisker edges represent the furthest point within 1.5 times the

interquartile range from the box, and the red bracket represents the densest part of the dataset that encompasses 50% of the data.

A mean for each individual was calculated and compared using a one-way ANOVA with Tukey HSD to understand if there were significant differences between standoffs in individuals. There were 10 significantly different ($p<0.0001$) groups of mean standoffs within the 25 individuals measured, where 4 individuals belonged to two groups (Figure 6). The range of the mean standoff values for individuals was 5.59 mm.

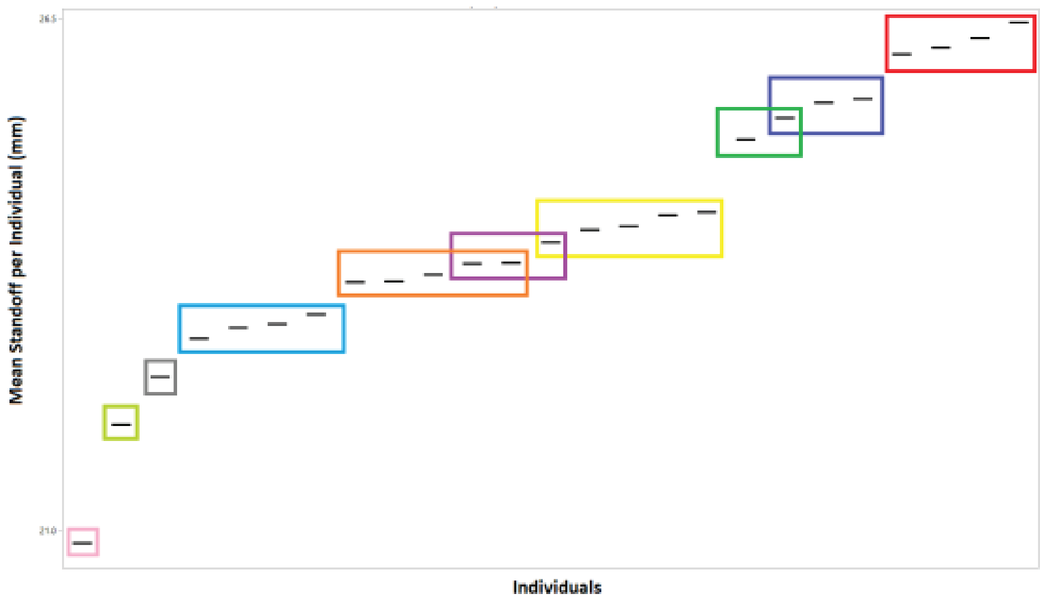

Figure 6: Mean standoff per individual in millimetres on Y-axis and each individual on X-axis, represented as a line, for comparison of statistically different groupings as highlighted by different color boxes.

3.3. Human Head Anthropometry

Anthropometric measurements were taken for length, breadth and circumference of each individual to understand the difference in human head anthropometry that is typically used for helmet fitting[5]. The range of head length was 167- 215 mm with an average of 187.72 ± 11.08 mm (Figure 7). The range of head breath was 119-170 mm with an average of 149 ± 12.91 mm. The range of head circumference was 538-591 mm with an average of 561.24 ± 15.32 mm. Calculated average eccentricity (length/breadth) was 1.27 ± 0.10 with a range from 1.07 to 1.45. These ranges may affect the standoff because of differences in helmet fit due to head shape. If the circumference is larger, then the expected standoff in that region would be less. Head length and breadth give a dimension of how circular or oblong the head shape would be at the measurement plane.

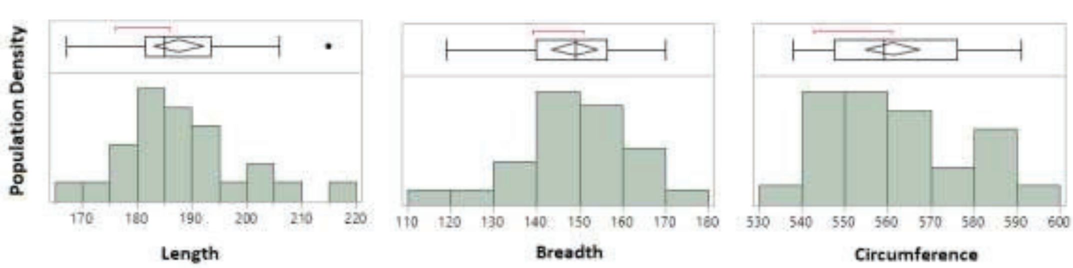

Figure 7: Distributions for head length, breadth and circumference in millimetres. Boxplot at the top of the graph represents the spread of data where the centre line is the 50% median, the middle of the

https://doi.org/10.52202/080042-0014

diamond is the sample mean with top and bottom indicating a 95% confidence interval, the whisker edges represent the furthest point within 1.5 times the interquartile range from the box, and the red bracket represents the densest part of the dataset that encompasses 50% of the data.

4. DISCUSSION

This study reported variation in standoff of helmeted human heads with a total dataset of over 104,000 standoff points for 25 individuals. It is to be noted that the individuals included in this study were from the United States and there may be differences in size and geometry depending on the region of origin [14, 18]. Furthermore, this study used a single helmet geometry, and other helmets might have different standoff distributions than the ones presented here. The standoffs that were measured in this study, in general, were larger than standoffs that have been previously reported in BHBT literature [2-5, 21]. The average reported standoff of the total dataset was 24.1 ± 4.5 mm. The individual averages ranged from 20.87 to 26.46 mm. While averages give an idea of a representative standoff value, it can be misleading to assume that the average standoff data encompasses the densest region of data as shown by the askew distributions and bimodal distributions of some of the human heads.

The reported ranges of the individual average standoffs and the 25%-75% quartile range for the total population from this study was around 6 mm. In the study of BHBT impacts by Deck et al, there was a distinct change in injury prediction from less serious at the 25 mm standoff to more serious at the 19 mm standoff, only with a difference in standoff of 6 mm [2]. Although these standoffs are smaller than the average standoffs identified in this study, this information indicates that standoff ranges as small as 6 mm can affect the predicted injury through energy transfer. In other words, for a single impact condition, the representative predictions from transferred energy for the population of potential wearers may not be captured by a single standoff.

There are some headforms that have been reverse engineered to have the same standoff at any location by matching helmet curvature to headform curvature [3]. This approach is reasonable if the purpose of the test is to only evaluate the material performance of the helmet but is not ideal for understanding the energy transfer from the helmet to head since it incorrectly assumes that a single standoff represents the fit of the helmet on the head. This approach also limits the application of the headform to helmets that may not have the same geometry as the helmet that the headform was designed for, resulting in more variation of future test results and an unequal comparison to previous test results.

There are other headforms that have been designed from human head anthropometric data [14, 15, 22, 23]. These headforms were designed for blunt impacts where energy transfer is correlated to the rigid-body motion of the head; therefore, the size parameters of these headforms prioritise factors associated with mass and moments of inertia. In other words, ensuring appropriate standoff in these headforms is not as important as ensuring proper kinematics. In BHBT impacts, the peak accelerations and bulk motion of the head occur hundreds and tens of thousands of microseconds after the peak loading [24], whereas standoff has been shown to play a significant role in energy transmission to the head [2-5]. Consequently, headforms to be used for BHBT evaluations should prioritize representing standoff over rigid-body motion.

Many helmets and headforms are sized using head circumference [5, 25]. However, in this study, the individual with the smallest circumference (and the other two anthropometric measurements) unexpectedly did not have the maximum recorded standoff value, though this individual was biased toward larger standoffs. Head circumference had a poor correlation ($R^2 = 0.15$) with mean standoff in this study, indicating that those with large head circumferences do not necessarily have smaller average standoffs (Figure 8). These findings suggest that circumference should not be the only component to consider when determining helmet fit.

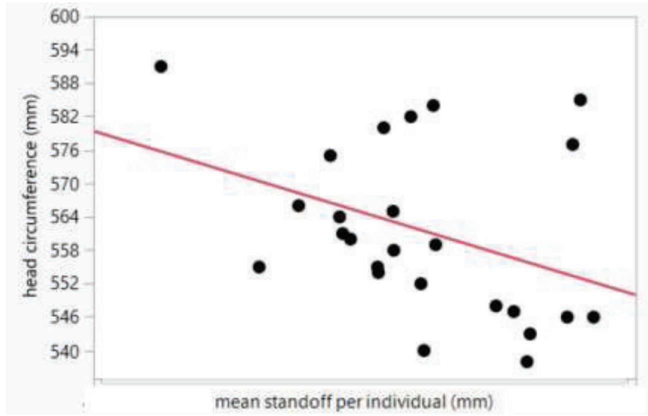

Figure 8: Comparison of head circumference in millimetres to mean standoff per individual in milimetres. The fit line (red) shows a poor correlation (R^2 value of 0.15) between mean standoff and head circumference.

Despite the same circumference of headforms, there are geometric differences that may affect standoff such as headform curvature, breadth, length and height from the reference plane [14]. The ratio of length and breadth, or eccentricity of the ellipse, describes how oblong or round a head may be and may provide insight into relevant head shapes for helmet fitting. Previous literature suggests that eccentricity be included in fit of helmets [17-19, 23] and consequently the standoff depending on shape. Eccentricity was calculated with the length and breadth values for each individual in this study, resulting in an average eccentricity of 1.27. Some existing headforms have a close-matching eccentricity value of 1.26 (Hybrid III 50th percentile), while others have different values such as 1.32 (NOCSAE and clay headform), 1.41 (ISO J), and 1.42 (DOT) [26, 27]. If implementing currently available headforms, the same helmet would inherently have different standoffs from the differences in eccentricity from these different headforms, potentially affecting the interpretation of the injury risk from results.

When exploring differences between individuals by fitting a density curve to the distribution, 92% had a platykurtic distribution and 96% of the population had a multi-peak distribution. The platykurtic distribution, or flatter distribution, suggests that extreme standoffs are not any less likely along the range of an individual. The multi-peak distribution implies that in a single individual there may be two or three distinct standoff distributions due to incompatibilities between the helmet and head geometries. For example, the four individuals with bimodal distributions had a shorter head height which led to the second peak from the larger standoffs measured in the crown region. This suggests that other anthropometric measurements including a parameter involving head height may be important to consider when fitting helmets and designing a headform for BHBT [17, 25, 28]. Additionally, only using a single-shape headform may not represent the fit of helmets on the soldier population since there are a wide array of head shapes [20, 28].

Behind helmet blunt trauma stems from the energy transfer of the helmet impacting the head after defeating the threat. The main purpose for helmets regardless of injury mechanism is to attenuate incoming energy, thereby, reducing or preventing injury. For BHBT specifically, some characterise the potential for head injury through recorded maximum depth on a clay headform [5, 27], measured energy transmission [1-3], measured force [29-31] or comparison to injuries sustained on PMHS [4, 9, 21, 32, 33]. For an accurate prediction of injury risk, an understanding of standoff variance is needed because of the effect on energy transfer.

Some helmet manufacturers choose to report the maximum depth of the ballistic transient deformation as a representative energy transfer metric because it is measured for body armour [34]; however, there is no reported correlation with head injury [5, 35]. Despite many issues that may affect the final depression in the clay headform [5], the intent is to statically capture the maximum displacement from a dynamic event to represent the differences in energy transfer behind the helmet. In the context of standoff, for a given impact condition, a larger standoff would decrease the measured maximum depth, indicating less energy transfer to the head. This reduction is due to the increased distance between the helmet and head allowing the helmet more space to dissipate the energy from the incoming threat before striking the head.

 https://doi.org/10.52202/080042-0014

Through this type of testing, some specific BFS maximums have been suggested based on comparison to other quantitative metrics from previous tests, however it is unknown if the standoffs from the previous experimental tests using other headforms match the standoff on the clay headform [5, 35].

Some BHBT impact experiments use instrumented PMHS that measure similar engineering metrics to headforms and compare outputs in other laboratory settings [4, 7, 9]. Headform dynamic responses are mechanically different compared to PMHS [14], therefore the data from PMHS provides an integral component to understanding human injury. If there is a different relative standoff when testing helmeted PMHS, as shown by the increased overall standoff average in this study to previously tested values, then the associated results may not provide accurate predictions when tested on headforms which typically have smaller standoff values. In a previous study investigating the effect of standoff without considering the influence of pads or helmet support,, a difference of 1.5 mm in standoff, changed the predicted injury risk from 2% to 100% [2]. Since this study clearly shows that the range of variance within standoff values for a helmeted human is well beyond 1.5mm, it may be prudent to compare equal standoff values to better understand risk when using a headform because there is larger than 2 mm difference between the largest headform standoff to the average value of this study.

5. CONCLUSIONS

Law enforcement officers require head protection that minimises the injury risk of BHBT. The variation between previously tested standoffs makes cross comparison of injury results problematic due to differences in input energy from the defeated threat. Standoff variation is a known issue for helmet testing [5], even with standardised headform geometry. With the addition of human biovariablity in head geometry, the standoff could be larger or smaller at different locations which affects predicted outcomes. Testing a single standoff may lead to unrealistic predictions.

Acknowledgments

The research reported in this document was performed in connection with contract/instrument W15P7T-19-D-0126 with the Combat Capabilities Development Command (DEVCOM) Army Research Laboratory. The findings in this report are not to be construed as an official Department of the Army position unless so designated by other authorised documents. The views and conclusions contained in this document are those of Bennett Aerospace Inc. and the DEVCOM Army Research Laboratory.

References

1. Hisley, D.M., J.C. Gurganus, and A.W. Drysdale, *Experimental methodology using digital image correlation to assess ballistic helmet blunt trauma.* Journal of Applied Mechanics, 2011. **78**(5): p. 051022.
2. Deck, C., et al. *Assessment of behind armour blunt trauma risk for a combat helmet by a combined experimental and numerical method*. in *PASS2018-14th Personal Armour Systems Symposium 2018, Washington, DC, USA, 1-5 October 2018*. 2018.
3. Miranda-Vicario, A., P. Bravo, and F. Coghe, *Experimental study of the deformation of a ballistic helmet impacted with pistol ammunition.* Composite Structures, 2018. **203**: p. 233-241.
4. Sarron, J.-C., et al., *Dynamic Effects of a 9 mm Missile on Cadaveric Skull Protected by Aramid, Polyethylene or Aluminum Plate: An Experimental Study.* Journal of Trauma and Acute Care Surgery, 2004. **57**(2): p. 236-243.
5. Council, N.R., *Review of Department of Defense test protocols for combat helmets*. 2014: National Academies Press.
6. DiChiara, A. and M. Addonizio, *Law Enforcement Advanced Protection (LEAP) Requirements Focus Group Report*. 2007, Army Natick Soldier Research Development and Engineering Center, MA.
7. Rafaels, K.A., et al., *Injuries of the head from backface deformation of ballistic protective helmets under ballistic impact.* Journal of forensic sciences, 2015. **60**(1): p. 219-225.
8. Freitas, C.J., et al., *Dynamic Response Due to Behind Helmet Blunt Trauma Measured with a Human Head Surrogate.* International Journal of Medical Sciences, 2014. **11**(5): p. 409-425.

9. Sarron, J.C., et al., *Consequences of nonpenetrating projectile impact on a protected head: study of rear effects of protections.* J Trauma, 2000. **49**(5): p. 923-9.
10. Palomar, M., et al., *Relevant factors in the design of composite ballistic helmets.* Composite Structures, 2018. **201**: p. 49-61.
11. Azevedo, A., F. Coghe, and F. Teixeira-Dias. *Behind Helmet Blunt Trauma: Matching Measurement to Injury Using Finite Element Modelling*. in *Advanced Materials for Defense: Development, Analysis and Applications*. 2020. Springer.
12. Kulkarni, S., et al., *Ballistic helmets–their design, materials, and performance against traumatic brain injury.* Composite Structures, 2013. **101**: p. 313-331.
13. Bass, C., B. Boggess, and B. Bush. *Ballistic Helmet Backface Deformation Testing with a Dummy Subject []*. in *Personal Armour Systems Symposium (PASS)*. 2000.
14. Bonin, S.J., et al., *Dynamic Response and Residual Helmet Liner Crush Using Cadaver Heads and Standard Headforms.* Ann Biomed Eng, 2017. **45**(3): p. 656-667.
15. Becker, E.B., *Helmet development and standards.* Biomedical and Health Research, Frontiers in Head and Neck Trauma. California: IOS press, 1998.
16. Hopping, J.A., et al., *Methodologies for blunt trauma assessment in military helmets*. 2010, Project Manager Soldier Protection and Individual Equipment Haymarket,VA.
17. Guo, F., L. Wang, and D. Dong. *Human head 3D dimensions measurement for the design of helmets*. in *International Conference on Digital Human Modeling*. 2009. Springer.
18. Luximon, Y., R. Ball, and L. Justice, *The 3D Chinese head and face modeling.* Computer-Aided Design, 2012. **44**(1): p. 40-47.
19. Meunier, P., et al., *Helmet accommodation analysis using 3D laser scanning.* Applied Ergonomics, 2000. **31**(4): p. 361-369.
20. Zhang, J., et al., *Customize my helmet: A novel algorithmic approach based on 3D head prediction.* Computer-Aided Design, 2022. **150**: p. 103271.
21. Rafaels, K., *Behind Helmet Blunt Trauma Experimental Impacts Using Ballistic Helmets*. 2017, CCDC ARL.
22. Hubbard, R. and D. McLeod, *A basis for crash dummy skull and head geometry.* Human impact response: measurement and simulation, 1973: p. 129-152.
23. Gilchrist, A., N. Mills, and T. Khan, *Survey of head, helmet and headform sizes related to motorcycle helmet design.* Ergonomics, 1988. **31**(10): p. 1395-1412.
24. Council, N.R., *Testing of body armor materials: Phase III*. 2012: National Academies Press.
25. Ellena, T., et al., *The Helmet Fit Index–An intelligent tool for fit assessment and design customisation.* Applied ergonomics, 2016. **55**: p. 194-207.
26. Cobb, B.R., A.M. Zadnik, and S. Rowson, *Comparative analysis of helmeted impact response of Hybrid III and National Operating Committee on Standards for Athletic Equipment headforms.* Proceedings of the Institution of Mechanical Engineers, Part P: Journal of Sports Engineering and Technology, 2016. **230**(1): p. 50-60.
27. Justice, N.I.o., *NIJ Standard for Ballistic Helmets* 1981. p. 13.
28. Oudenhuijzen, A. and F. ter Haar, *Digital Head Avatars for combat helmet fit.* 2018.
29. Anctil, B., et al. *Evaluation of impact force measurement systems for assessing behind armour blunt trauma for undefeated ballistic helmets*. in *PASS conference proceedings, Edited by J Van Bree, The Hague, The Netherlands, September*. 2004.
30. Aranda, R., et al. *Integrated Assessment of Ballistic Backface Deflections on Combat Helmets and Prediction of Injury Risks*. in *31st International Symposium on Ballistics*. 2019.
31. Grobert, S., et al. *Comparative Investigations on Ballisitc Backface Deflections of Combat Helmets Using Force Measurement and Digital Image Correlation*. in *32nd International Symposium On Ballistics*. 2022.
32. Raymond, D., et al., *Tolerance of the skull to blunt ballistic temporo-parietal impact.* Journal of Biomechanics, 2009. **42**(15): p. 2479-2485.
33. Matheis, E., A. Eidsmore, and K. Rafaels, *Ballistic Factors of Behind Helmet Blunt Trauma Skull Fracture*, in *31st Annual International Ballistics Symposium*. 2019: Hyderabad, India.
34. Greene, M., et al. *The Next Revision of the NIJ Performance Standard for Ballistic Resistance of Body Armour, NIJ Standard 0101.07: Changes to Test Methods and Test Threats*. in *Personal Armour Systems Symposium PASS 2018 Proceeding Book*. 2018.
35. Young, L., et al., *When physics meets biology: low and high-velocity penetration, blunt impact, and blast injuries to the brain.* Frontiers in neurology, 2015. **6**: p. 89.

 https://doi.org/10.52202/080042-0014